Journal of Glaciology

Article

Cite this article: Rendfrey TS, Bassis J, Pettersen C (2025). Do atmospheric rivers trigger tabular iceberg calving? *Journal of Glaciology* **71**, e8, 1–12. https://doi.org/10.1017/jog.2024.94

Received: 17 July 2024
Revised: 12 November 2024
Accepted: 18 November 2024

Keywords:
ice shelves; ice/atmosphere interactions; ice-shelf break-up; iceberg calving

Corresponding author:
Tristan Rendfrey;
Email: rendfrey@umich.edu

cambridge.org/jog

Do atmospheric rivers trigger tabular iceberg calving?

Tristan Scott Rendfrey, Jeremy Bassis and Claire Pettersen

Department of Climate and Space Sciences and Engineering, University of Michigan-Ann Arbor, Ann Arbor, MI, USA

Abstract

The processes governing iceberg calving from ice shelves remain poorly understood. Recent studies suggest that anomalous atmospheric moisture transport events – atmospheric rivers – can act as triggers for calving. These conclusions, however, were based on studies of case studies of individual icebergs or ice shelves, making it difficult to determine if this relationship remains apparent when considering a wider set of calving events and ice shelves. Here, we assemble an Antarctic-wide catalog of tabular iceberg calving events to evaluate whether a significant correlation exists between calving and enhancement of total and meridional integrated vapor transport (IVT), a measure of atmospheric moisture transport. We find that ~80% of the calving events in our study occur when metrics of IVT are less than the 90th percentile of their monthly climatologies. However, the remaining ~20% of calving events that occur during periods with short-term enhanced IVT exhibit a statistically significant correlation. The results, however, are regionally dependent, with a statistically significant correlation between enhanced IVT and calving in the Antarctic Peninsula and none in the Amundsen Sea Embayment. This suggests that, although enhanced IVT is not a primary control on the iceberg calving process, enhanced IVT may play a role in triggering calving events under certain conditions.

Introduction

Freely floating ice shelves surround much of the Antarctic ice sheet, where they serve as the primary sources of ice mass discharged into the ocean (Dupont and Alley, 2005). Antarctic ice shelves also provide a buttressing stress on grounded ice (e.g. Dupont and Alley, 2005; Goldberg and others, 2009; Gagliardini and others, 2010; Gudmundsson, 2013; Miles and others, 2022) that reduces mass flux across ice-shelf grounding lines. Buttressing from ice shelves therefore slows dynamic discharge from the Antarctic ice sheet and stabilizes it from irreversible retreat associated with marine ice sheet and, potentially, marine ice cliff instability (Bassis and Walker, 2011; Pollard and others, 2015; DeConto and Pollard, 2016; Edwards and others, 2019; Garbe and others, 2020; Bassis and others, 2024).

Mass loss from ice shelves can decrease their ability to buttress upstream ice (Paolo and others, 2015; Rignot and others, 2019). The process of mass loss from ice shelves is primarily controlled by a combination of basal melting and iceberg calving (e.g. Liu and others, 2015). Observations currently show roughly equal magnitudes of basal melt and iceberg calving contributions to the total mass loss from the entire Antarctic ice sheet (e.g. Depoorter and others, 2013; Liu and others, 2015; Greene and others, 2022), although the partition between the amount of mass lost to basal melt and calving is highly variable between ice shelves (Liu and others, 2015; Davison and others, 2023). Currently, mass loss due to surface melt is small over most Antarctic ice shelves (Kuipers Munneke and others, 2012; Lenaerts and others, 2019). However, surface melt has been implicated in the hydrofracture-related explosive collapse of the Larsen B Ice Shelf, which occurred unexpectedly in 2002 following a period of melt pond formation (van den Broeke, 2005; Glasser and Scambos, 2008; Banwell and others, 2013).

Although surface and basal melting are directly controlled by both atmospheric and oceanic forcing, the overall processes controlling iceberg calving remain poorly understood (e.g. Lazzara and others, 1999; Walker and others, 2015, 2021; Benn and others, 2022; Alley and others, 2023; Bassis and others, 2024). Unlike the spectacular disintegration of the Larsen B Ice Shelf, the calving process from most ice shelves occurs through the initiation and propagation of rifts – fractures that penetrate the entire ice shelf thickness, which can propagate on timescales up to decades (e.g. Bassis and others, 2008; Walker and others, 2013; Lipovsky, 2020). Rift-propagating processes contribute to the calving of tabular icebergs when they result in the separation of an area of ice from the rest of the shelf (Lazzara and others, 1999; Joughin and MacAyeal, 2005; Kenneally and Hughes, 2006; Indrigo and others, 2020). Tabular icebergs, which can exceed hundreds of kilometers in length, remove mass near-instantaneously from the Antarctic ice sheet (Lazzara and others, 1999; Joughin and MacAyeal, 2005) and are the primary mode of calving from ice shelves (Fricker and others, 2002; Bassis and others, 2008, 2024).

The tabular iceberg calving process has traditionally been thought to be primarily controlled by the internal stress within the ice shelves (Robin, 1979; Bassis and others, 2008; Amundson and Truffer, 2010; Humbert and Steinhage, 2011; Bassis and Jacobs, 2013; Walker and others, 2015; Indrigo and others, 2020). However, studies have also indicated

external stress from tidally-induced currents (Legrésy and others, 2004; Lescarmontier and others, 2015) and pulses of ocean swell (MacAyeal and others, 2006; Bromirski and others, 2010; Sergienko, 2010) as triggers for calving. Alternatively, unusually large sea surface slopes have also been hypothesized to induce rift propagation on Antarctic ice shelves (Mayet and others, 2013; Francis and others, 2021). However, the physical connection between these environmental triggers can be difficult to identify, as Bassis and others (2008) demonstrated that the stresses imposed on the ice are associated with many of these environmental forcings is much smaller than the internal stresses within the ice.

Recently, tabular iceberg calving events from the Larsen A, B and C ice shelves, the Amery Ice Shelf, the Brunt Ice Shelf and the Conger Ice Shelf have been linked to unusually strong poleward atmospheric moisture transport (i.e. atmospheric rivers; Francis and others, 2021, 2022; Laffin and others, 2022; Wille and others, 2022, 2024). In particular, Wille and others (2022) found that 60% of calving events from the Larsen A, B and C ice shelves were triggered by atmospheric rivers. It is, however, unclear if these findings generalize to other ice shelves in other regions. These atmospheric moisture transport extremes also correlate with many other potential triggers, including sea ice clearing and large sea surface slopes (Massom and others, 2018; Dziak and others, 2019; Francis and others, 2021, 2022; Wille and others, 2022, 2024). Moreover, the warm and moist atmospheric conditions and radiative effects associated with atmospheric rivers are directly related to surface meltwater formation on the ice shelves, which could make ice shelves more vulnerable to hydrofracture-induced collapse (Turton and others, 2020; Clem and others, 2022; Laffin and others, 2022; Wille and others, 2022).

Determining the potential relationship between the timing of iceberg calving events and enhanced atmospheric moisture transport, however, remains challenging. Although some calving events may coincide with elevated atmospheric integrated vapor transport (IVT), it is possible that this relationship is spurious, resulting in false correlations. This is especially true for regions where enhanced atmospheric moisture intrusions occur relatively often compared to the frequency of calving events. Moreover, although studies of individual ice shelves can avoid some of the issues around false attribution, they may not reveal heterogeneous behavior of ice shelves in different glaciological or climatological regimes. For example, the Antarctic Peninsula is located relatively far North compared to the Amundsen Sea Embayment, with some ice shelves experiencing surface melt (van den Broeke, 2005; Kuipers Munneke and others, 2018). By contrast, the Amundsen Sea Embayment ice shelves are located in regions with cold atmospheric conditions compared to the Antarctic Peninsula and experience little surface melt (Trusel and others, 2013). Both the Antarctic Peninsula and Amundsen Sea ice shelves, however, are located in regions where previous studies have documented synoptic-scale conditions that favor enhanced moisture transport (Nicolas and Bromwich, 2011; Wille and others, 2021; Swetha Chittella and others, 2022). Studies further provide evidence that elevated atmospheric moisture transport might trigger calving from the Antarctic Peninsula (Laffin and others, 2022; Wille and others, 2022).

Here, we seek to expand upon results from previous case studies and work focused on calving from the Antarctic Peninsula by examining if links between enhanced moisture transport and calving hold across a broader set of events from all Antarctic ice shelves. We use this extended dataset to see if there are regional differences in sensitivity to atmospheric moisture transport, and to determine when atmospheric moisture transport exhibits a statistically significant correlation with the timing of iceberg calving.

Data and methods

We first constructed a catalog of iceberg calving events, focusing on large 'tabular' icebergs with a characteristic length much larger than the ice thickness (e.g. Lazzara and others, 1999; Budge and Long, 2018). We then examined the monthly climatology of total and meridional moisture transport over each Antarctic ice shelf with a tabular iceberg calving event. This monthly climatology allowed us to assess the number of calving events that were preceded by enhanced moisture transport over each individual shelf. Finally, we tested if the relationship between enhanced moisture transport and the timing of iceberg calving is statistically significant using a bootstrap (Efron, 1979). We describe each step in this process in more detail below.

Catalog of tabular iceberg calving events

US National Ice Center named tabular icebergs

To construct our catalog of tabular iceberg calving events, we used the US National Ice Center (USNIC; usicecenter.gov) press releases. These press releases document new icebergs, including the location of where the new iceberg was first sighted, as well as the date of first sighting, the size and the ice shelf from which the iceberg detached. We use USNIC press releases that document all icebergs sighted between November 2013 and December 2023 with a longest side length >7 nautical miles or a total area >20 nautical miles squared (https://usicecenter.gov/Products/AntarcIcebergs). This detection method excludes the many smaller icebergs that can detach from ice shelves and glaciers, allowing us to focus on the processes governing the detachment of large tabular icebergs that feature prominently in the calving cycle of most ice shelves (Alley and others, 2023; Bassis and others, 2024).

MODIS image analysis of calving event timing

Determining the timing of iceberg calving required more information than we could attain from the USNIC press releases alone, both because they are issued after a calving event occurs and the reported timing of iceberg detachment is limited by the weekly timing of press releases. To more precisely identify the timing of iceberg detachment, we additionally examined satellite images from the Moderate Resolution Imaging Spectroradiometer (MODIS) instrument. We accessed images of iceberg calving viewed by the MODIS instruments from the Aqua and Terra satellites (Xiong and Barnes, 2006) using NASA WorldView (worldview.earthdata.nasa.gov). The Aqua and Terra satellites view the same point on Earth ~3 h apart (Crosson and others, 2012), therefore we had two images available for each day from 2013 to 2023. MODIS visible images have been previously used to determine calving event timing (e.g. Wille and others, 2022). Here, we examined MODIS images using the true-color visible imagery (0.45–0.67 µm wavelength; 500 m spatial resolution) during seasons with available sunlight (approximately October through April) over the iceberg or ice shelf. For seasons without sufficient sunlight (approximately April through October), we used the MODIS infrared channels (10.780–11.280 µm wavelength) to distinguish between the ice shelves, icebergs and ocean. The MODIS infrared brightness temperatures allow for detection of the icebergs, but have lower spatial resolution than the visible channels (1 km). However, because we were only focused on tabular icebergs that are much larger in size than 1 km^2, the lower resolution in the infrared does not affect our ability to detect iceberg calving detachment events.

We determined the timing of iceberg calving by combining the information from MODIS and USNIC press releases in the following way, illustrated in Figure 1: we first examined the USNIC press release (Fig. 1a) for a date and the location to begin viewing the MODIS visible and/or infrared images over

https://doi.org/10.1017/jog.2024.94 Published online by Cambridge University Press

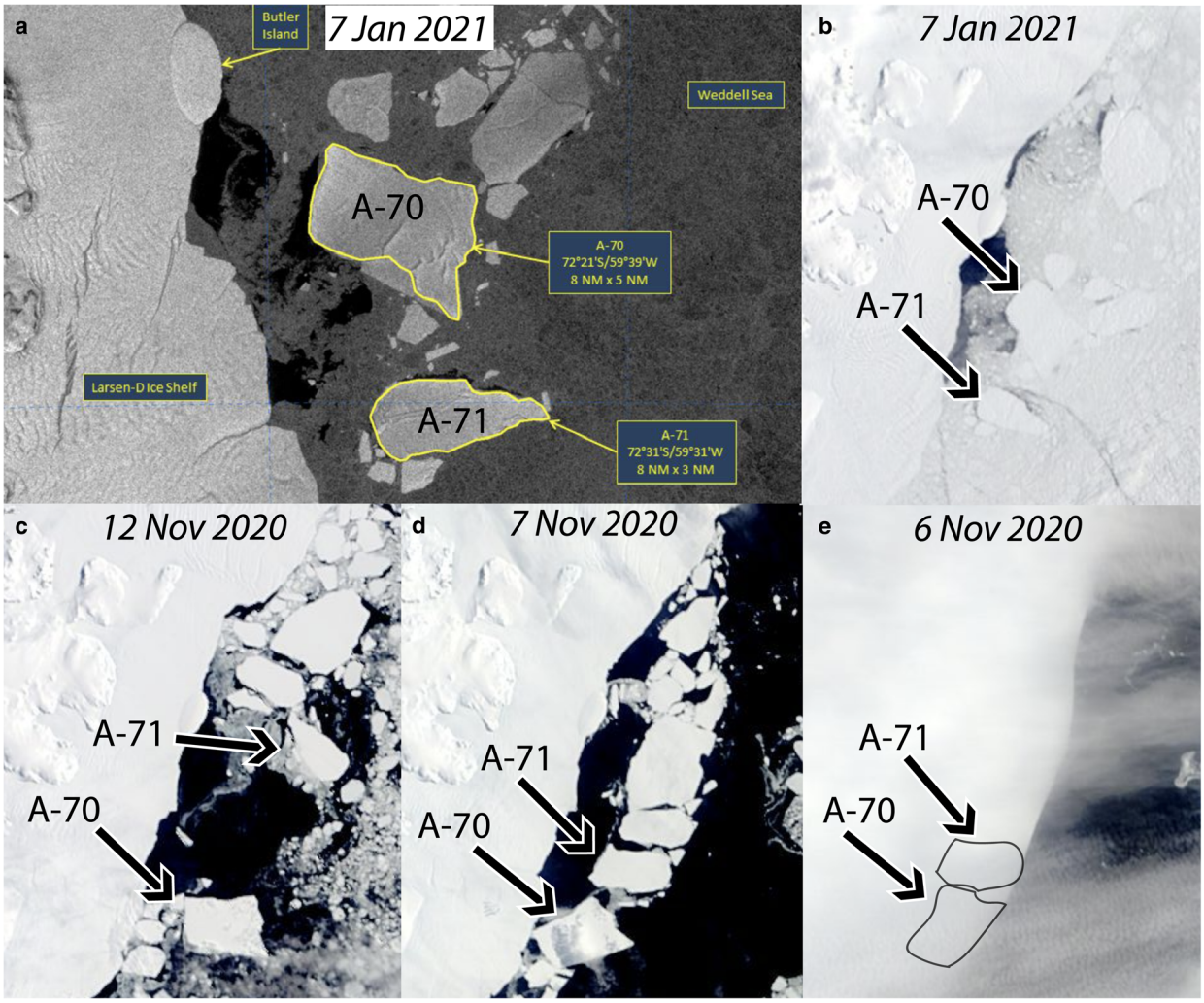

Figure 1. An example of the process used to determine iceberg calving dates. (a) Example showing an image of icebergs A-70 and A-71 from 7 January 2021 provided by the USNIC press release for the icebergs issued on 8 January. (b) The same scene viewed by MODIS, including the Larsen D Ice Shelf. (c) MODIS image of the Larsen D Ice Shelf on 12 November 2020, 8 d before calving, which was used as part of the sequence that tracked the icebergs from 7 January 2021 back to the calving date. (d) MODIS image on day of calving icebergs A-70 and A-71 (and smaller unnamed icebergs). (e) MODIS image of the ice shelf 1 d prior to the calving event. In this panel, indications of the outlines of the ice shelf areas that will calve into icebergs A-70 and A-71 are shown.

the iceberg (Fig. 1b). We then obtained the MODIS imagery of the same scene for the previous day, and re-centered the image on the iceberg to account for drift in the open ocean waters (e.g. Fig. 1c). We repeated this process, stepping back 1 d and re-centering the image on the iceberg (e.g. Fig. 1d), until the iceberg appears to be attached to an ice shelf (Fig. 1e). We identified the first day of images that show the detachment of the iceberg from the shelf as the 'calving event' and the day of the image as the time of the event. An important caveat to our method is that our catalog was determined using the date when icebergs start to drift away from their parent ice shelf, which may occur after some time after rifts first isolate an iceberg, especially if icebergs are surrounded by fast ice or melange (e.g. Schlemm and Levermann, 2021; Alley and others, 2023). Cloudy conditions may also obscure the view of the ice surface in both visible and infrared images. This introduced an uncertainty in the calving event timing that is equal to the number of days in a cloudy period during iceberg detachment. This uncertainty was <2 d for 29 of the 41 events (70% of the calving events) and up to 5 d for 12 of the events (30% of the calving events).

Catalog of tabular iceberg calving events

To focus on the atmospheric drivers of calving, we removed icebergs from our catalog that formed through fragmentation or fracture of existing floating icebergs (e.g. England and others, 2020). For the same reason, we also removed the entries for icebergs that detached due to collisions between ice shelves and already-floating icebergs. This removed two iceberg detachments. Additionally, following previous case studies that argued that the cumulative effect of moisture transport was the trigger for calving (e.g. Francis and others, 2021, 2022), we then examined running averages of atmospheric variables over 7 and 28 d prior to each calving event (see next section for details). Consequently, if an iceberg calved from the same ice shelf in the 28 d prior to an identified event, we removed the iceberg that calved later from the catalog to preserve the independence of the 28 d running average. This method removed one iceberg from the Conger Ice Shelf (C-38) and one from the Pine Island Ice Shelf (B-36) from the catalog. Finally, if multiple icebergs detach from the same ice shelf on the same day, we consider them as a single calving event. We made these decisions to avoid the potential to overestimate the influence of atmospheric drivers if multiple calving events are correlated with the same atmospheric event. We found that the statistical significance of our results, however, was insensitive to these omissions.

Our final catalog included 41 tabular iceberg calving events over a total of 23 ice shelves. We noted that 13 calving events came from ice shelves located in the Amundsen Sea Embayment (defined as

https://doi.org/10.1017/jog.2024.94 Published online by Cambridge University Press

the Pine Island, Thwaites, Dotson and Getz ice shelves), and eight calving events came from Antarctic Peninsula ice shelves (defined as the Larsen C, D, F and George VI ice shelves).

Atmospheric moisture transport analysis over Antarctic ice shelves

ERA5 reanalysis

To assess atmospheric moisture transport over Antarctic ice shelves prior to the calving events in our catalog, we examined variables using the ECMWF fifth-generation atmospheric reanalysis (ERA5; Hersbach and others, 2020). ERA5 has a spatial grid of 0.25° resolution, and we used a 3 hourly temporal resolution. We focused here on the vertically IVT, a common measure used to quantify moisture transport. IVT measures the flux of water vapor through a column of the atmosphere, which depends on the water vapor content of and wind speed through the column. IVT therefore can be expressed in units of kg m^{-1} s^{-1}. Very high values of IVT in a narrow enough region are traditionally used to characterize atmospheric rivers (e.g. Gimeno and others, 2014; Wille and others, 2019). Because atmospheric moisture originates in the tropics and is then transported poleward, atmospheric river detection has often focused on the intensity of poleward-directed IVT (the meridional component of IVT, e.g. Wille and others, 2019). The zonal component describes easterly or westerly-directed IVT, and accounts for moisture transport events that are not purely in the poleward direction. Some studies (e.g. Bozkurt and others, 2022) use total IVT, which is equal to the magnitude of the IVT vector and is calculated from the sum of the squares of the zonal and meridional components of IVT. To account for the different definitions, we adopt both metrics of IVT to investigate the influence of water vapor transport on iceberg calving from ice shelves. We calculate the total IVT from the zonal (IVT^U) and meridional components of the IVT vector (IVT^V), both obtained from the ERA5 reanalysis. We calculated the total IVT, or the magnitude of the IVT vector (denoted IVT^T) from the components according to $IVT^T = \sqrt{(IVT^U)^2 + (IVT^V)^2}$. In addition to IVT^T, we examined IVT^V, which is linked to the strength of moisture transport across the midlatitudes toward the polar regions, both poleward and equatorward (Bozkurt and others, 2018; Nash and others, 2018; Shields and others, 2022). Both IVT^T and IVT^V have been used to characterize atmospheric rivers over Antarctica (e.g. Gorodetskaya and others, 2014; Adusumilli and others, 2021; Terpstra and others, 2021; Wille and others, 2021; Gorodetskaya and others, 2023; Maclennan and others, 2023; Rendfrey and others, 2024).

Averaging IVT over ice shelves' bounds

To evaluate the atmospheric moisture transport conditions over the ice shelves preceding calving events, we used the ice shelf bounds from Mouginot (2017) for the ice shelves in our catalog. Changes in ice shelf area from the years 2007–09 included in the study of Mouginot (2017) are relatively small for ice shelves included in our study and do not affect the ERA5 points included in the ice shelf bounds. We then computed the spatial average of total IVT (IVT^T) and the meridional IVT (IVT^V) for every 3 h time step available in the ERA5 data. To do this, we selected the ERA5 grid points that are contained within each ice shelf's respective boundary (Fig. 2a). We then used those gridpoints to compute the spatial average of IVT^T and IVT^V over each ice shelf. Because there is a large range of sizes among the ice shelves, the number of ERA gridpoints per ice shelf varies. The latitudes and longitudes corresponding to the ERA5 gridpoints used for each ice shelf are given in Excel Table S2 in the Supplementary material.

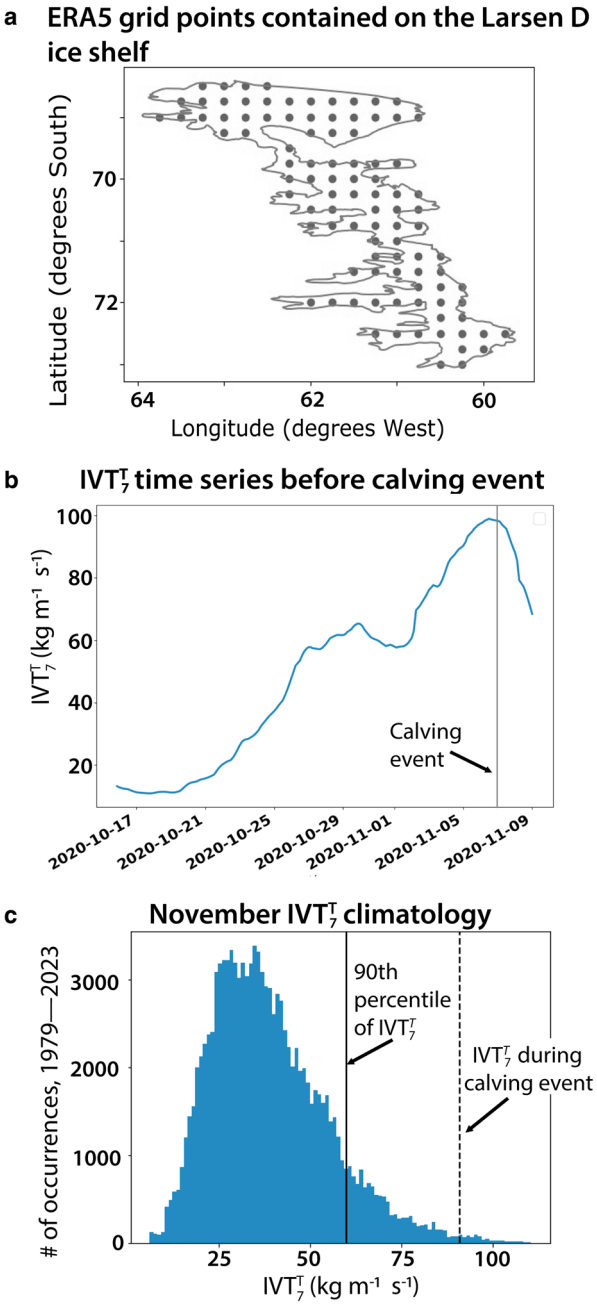

Figure 2. Steps of the described method displayed graphically for the 7 November 2020 calving event from Larsen D as an example. (a) ERA5 gridpoint selection within the bounds of the Larsen D Ice Shelf. (b) A time series of IVT_7^T prior to the example calving event. (c) An example of the November climatology of IVT_7^T from 1979 to 2023 for the Larsen D Ice Shelf. The *Y*-axis values correspond to the number of occurrences for each binned value of IVT_7^T in November months between 1979 and 2023. Vertical lines show the 90th percentile of the November IVT_7^T distribution for 1979–2023 and the value of IVT_7^T for the example calving event.

Short-term and long-term temporal IVT averages

We next calculated 7 and 28 d running averages of the variables for each 3 h time step in the ERA5 climatology after we averaged the variables spatially within the ice-shelf bounds. We chose the 7 d rolling mean for each ice shelf as a 'short-term' timescale to align with the 5 d cumulative IVT analyzed by Wille and others (2022); however, we included two additional days to account for the uncertainty in our calving event date estimation methodology. We chose a 28 d rolling mean for the 'long-term' influence based on case studies of iceberg calving from the Brunt and Amery ice shelves (e.g. Francis and others, 2021, 2022). We denote the 28 d running average of IVT^T and IVT^V with the variables IVT_{28}^T and

https://doi.org/10.1017/jog.2024.94 Published online by Cambridge University Press

IVT^V_{28}, respectively. Similarly, we denote the 7 d running average of IVT^T and IVT^V with the variables IVT^T_7 and IVT^V_7 (see Fig. 2b for an example of IVT^T_7 before a calving event). We also analyzed 14 d running averages, but results from the 14 d averages were similar to the 7 and 28 d and did not provide additional insight. We generally refer to the results of these computations, IVT^T_{28}, IVT^T_7, IVT^V_{28} and IVT^V_7, as the metrics of IVT. We also more specifically refer to IVT^T_{28} and IVT^V_{28} jointly as the 28 d metrics of IVT, and likewise the IVT^T_7 and IVT^V_7 as the 7 d metrics of IVT.

Statistical significance of correlations

Climatology and definition of enhanced IVT

We first determined the climatology of our four metrics of IVT over as long of a period available from the ERA5 reanalysis, which is between 1979 and 2023. The climatologies were computed independently for each ice shelf and for each month. Because IVT does not follow a normal distribution, we created histograms of the metrics of IVT for each of the monthly climatologies for each ice shelf. We used monthly climatology to be consistent with previous studies (e.g. Wille and others, 2022, 2024). It is possible to instead determine extreme events based on the annual climatology. This results in fewer calving events that are identified as coincident with extreme IVT and reduces the statistical significance of the association. We then defined 'enhanced IVT' with respect to each of our four metrics of IVT (IVT^T_{28}, IVT^T_7, IVT^V_{28} and IVT^V_7) as any value that exceeded the 90th percentile of the monthly climatology for each ice shelf (Camuffo and others, 2020) (an example of an event with enhanced IVT^T_7 is illustrated in Fig. 2c). We then counted the number of calving events in the catalog that have enhanced IVT for the four metrics for each ice shelf (IVT^T_{28}, IVT^T_7, IVT^V_{28} and IVT^V_7).

Estimating the statistical significance between IVT and calving events

To test the possibility that the timing between calving events and IVT is coincidental, we performed a bootstrap analysis (Efron, 1979). The bootstrap seeks to determine the probability that enhanced metrics of IVT are associated with calving events simply by random chance. We estimated this probability as follows: for each calving event in our catalog, we used a random number generator to choose a date from the same month and ice shelf location as the observed calving event between 1979 and 2023. We called this a 'synthetic event'. One iteration of this process produces 41 synthetic events drawn from the same ice shelves (and months) as the observed set of calving events. We then computed the four metrics of IVT for each synthetic event in the synthetic set to determine which (if any) of our metrics for IVT are enhanced. This provides a synthetic catalog of calving events where a fraction of the synthetic calving events are associated with one or more of our metrics for enhanced IVT purely by chance. We then repeated this process for 10 000 iterations to produce 10 000 sets of 41 synthetic events.

To estimate the probability that the observed association occurred purely by chance, we compared the number of observed calving events with enhanced metrics of IVT against the fraction of our synthetic sets that contained an equal or greater number of synthetic calving events with enhanced metrics of IVT. We did this calculation separately for each of our four metrics of IVT. For example, if our catalog had ten calving events and three of those calving events were associated with enhanced IVT^V_7, we would calculate the fraction of synthetic sets that have three or more calving events with enhanced IVT^V_7. If the fraction of synthetic events was, say, 20%, then there is a 20% chance that the three events observed were associated with enhanced IVT^V_7 by random chance alone. We defined statistical significance using the standard 95% confidence interval (Wilks, 2011). Hence, we considered the relationship between enhanced IVT and the timing of calving events to be statistically significant if an equal or greater number of synthetic events associated with enhanced metrics of IVT than calving events occurs in 5% or fewer of our 10 000 iterations. An important caveat is that our bootstrap assumed metrics of IVT could be treated as stationary stochastic processes. If climate change has led to more frequent or more intense moisture transport in more recent decades, as some studies suggest (e.g. Espinoza and others, 2018; Payne and others, 2020), our bootstrap could slightly overstate the significance of enhanced IVT.

Study regions

We applied our bootstrap to the entire, Antarctic-wide, catalog of calving events. However, given the different glaciological and climatological environments experienced by ice shelves across the Antarctic ice sheet, it is possible that certain regions – or ice shelves – are more sensitive to enhanced moisture transport than others. For this reason, we also performed the bootstrap for calving events in two regions of interest: the Amundsen Sea Embayment and Antarctic Peninsula. Ice shelves in these two regions have sufficient calving events for regional statistics, but also experience climate forcing from both the ocean and atmosphere. The Amundsen Sea Embayment experiences colder atmospheric conditions in its southerly location (Rignot, 2002; Trusel and others, 2013), while the more northerly Antarctic Peninsula ice shelves experience warmer near-surface air temperatures, which can cause widespread surface melt (Costi and others, 2018; Kuipers Munneke and others, 2018).

Results

Iceberg calving event timing

Our catalog of tabular calving events includes 41 events from 23 ice shelves. Calving events occurred during each month of the year and from different portions of the Antarctic ice sheet (Fig. 3). The largest number of events occurred during Austral summer (14 in December, January, February), whereas the fewest occurred during Austral winter (five in June, July, August). We see nine events during March, April and May and ten events during September, October and November. The majority of ice shelves in our catalog experienced two or fewer calving events; only the Pine Island (seven events), Larsen D (five events), Getz (four events) and Ninnis (three events) ice shelves experienced more than two events. The tabular icebergs in our catalog range in size from ~70 up to 7000 km^2 in surface area at the time of calving. Excel Table S1 in the Supplementary material contains the calving dates, their respective ice shelves, the size of the icebergs and the location of the iceberg at detection, as well as a link to the original USNIC press report.

Are calving events associated with enhanced values of 28 d IVT?

We first examined the two 28 d metrics of IVT (IVT^T_{28} and IVT^V_{28}) to determine if the timing of the calving events in our catalog are associated with longer-term synoptic scale forcing from IVT. Figure 4 shows the fraction of calving events from each ice shelf that are coincident with enhanced 28 d metrics of IVT. We find that 35 of the 41 (85%) calving events occurred during times when neither 28 d metric of IVT was enhanced. Conversely, we find that, for both IVT^T_{28} and IVT^V_{28}, 6 out of the 41 (15%) calving

https://doi.org/10.1017/jog.2024.94 Published online by Cambridge University Press

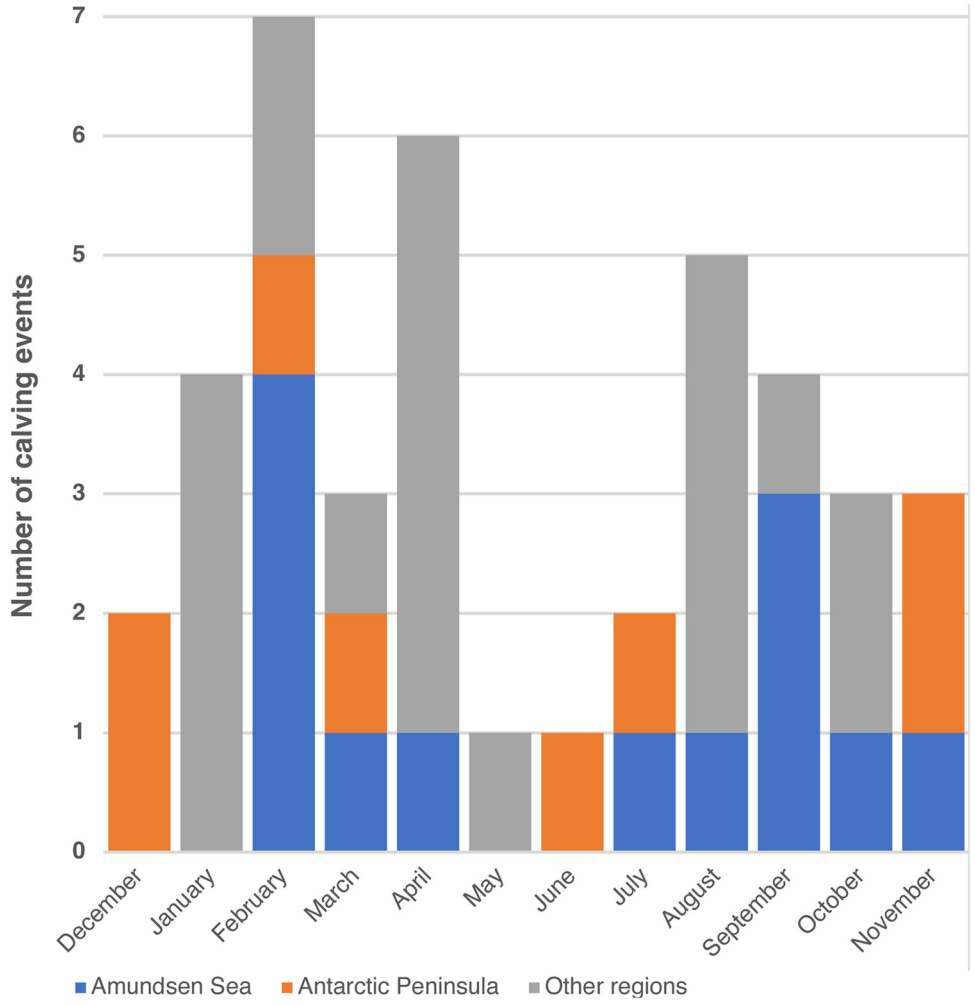

Figure 3. Number of calving events in the catalog in each month. The number of calving events in the Amundsen Sea Embayment (in orange) and Antarctic Peninsula (in blue) are presented along with the number of calving events from all other regions of Antarctica (in gray).

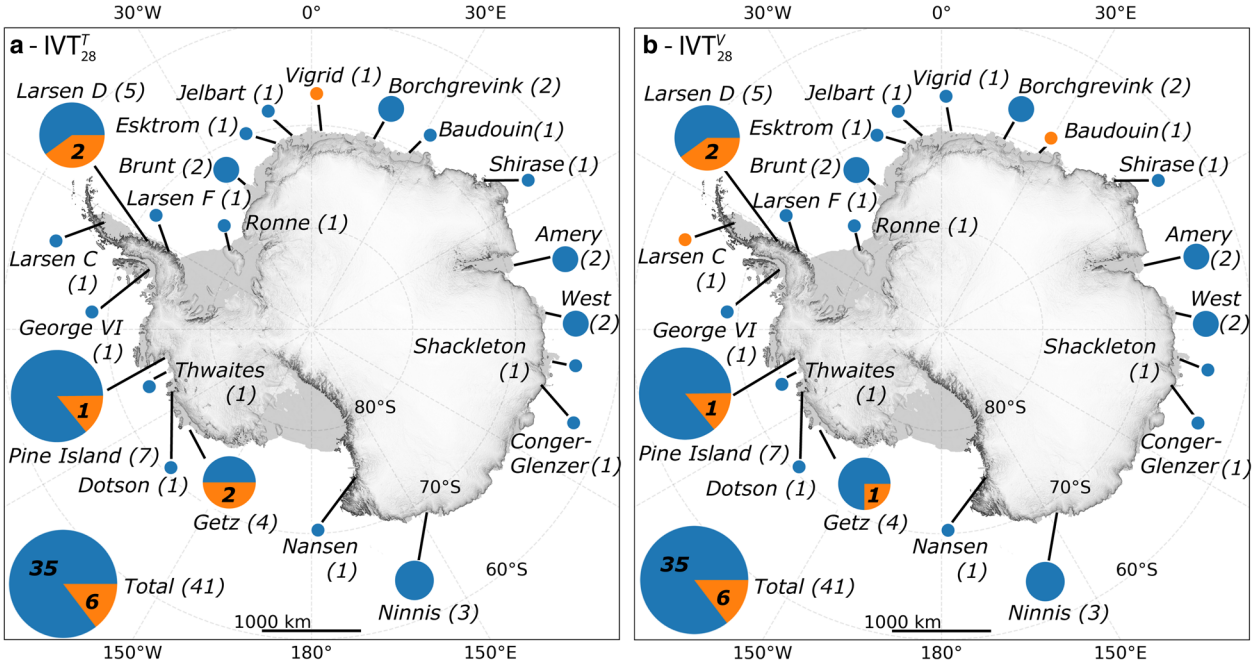

Figure 4. Calving events per ice shelf with the fraction of events that have enhanced 28 d IVT, shaded in orange, for (a) total IVT magnitude, IVT^T_{28}, and (b) meridional IVT, IVT^V_{28}. The radius of each circle is proportionate to the total number of calving events from the ice shelf associated with it. The total number of calving events from each ice shelf is listed beside the label for each circle. The numbers in each orange region are the counts of events with enhanced IVT^T_{28} or IVT^V_{28}. The total number of calving events is shown boxed in the lower left corner.

https://doi.org/10.1017/jog.2024.94 Published online by Cambridge University Press

events did occur when the metrics of IVT were enhanced. The calving events with enhanced 28 d are primarily located at the Larsen D, Getz, Pine Island, Vigrid and Baudouin ice shelves. However, despite the similarity in total numbers of events associated with the enhanced 28 d metrics of IVT, there are slight differences in the calving events that are identified as being associated with enhanced IVT^{T}_{28} and IVT^{V}_{28}. For example, the calving event from the Baudouin Ice Shelf is associated with enhanced IVT^{V}_{28}, but not IVT^{T}_{28}, whereas the calving event from the Vigrid Ice Shelf has enhanced IVT^{V}_{28}, but not IVT^{T}_{28}. This indicates that there is some sensitivity in our results to the metrics used.

Are calving events associated with enhanced 7 d IVT?

We next analyzed the relationship between calving and enhanced IVT^{T}_{7} and IVT^{V}_{7} (Fig. 5). Similar to the 28 d metrics of IVT, the majority of calving events are not associated with enhanced 7 d metrics of IVT (32 out of 41 or 78%). However, we see a larger number of calving events that are associated with enhanced 7 d metrics of IVT (9 out of 41) compared to the 28 d metrics of IVT (6 out of 41). We again see slight differences between the calving events associated with enhanced 7 d metrics of IVT. Here, the Larsen C and Ninnis ice shelves have calving events associated with enhanced IVT^{V}_{7}, but not IVT^{T}_{7}, whereas the Ekstrom and George VI ice shelves had a calving event associated with enhanced IVT^{T}_{7}, but not IVT^{V}_{7}. Overall, the ice shelves that had calving events associated with enhanced IVT^{T}_{7} or IVT^{V}_{7} are similar to those that had calving events associated with enhanced IVT^{T}_{7} or IVT^{V}_{7}, with the exception of calving events from the Ekstrom and Amery ice shelves that are associated with enhanced 7 d but not 28 d IVT. Hence, the 7 d metrics of IVT results in more calving events associated with enhanced IVT from a larger number of ice shelves than the 28 d metrics of IVT.

Is the association between enhanced IVT and calving events statistically significant?

Despite the fact that most calving events are not associated with enhanced values of any of our four metrics of IVT, we do find that 6 or 9 of the 41 calving events are correlated with one or more metrics of enhanced IVT (depending on the metric used). To determine if these numbers of events are statistically significant, we performed a bootstrap on the calving events in our catalog (see also the description in the Methods). When our bootstrap is applied to all calving events in our catalog, we find no statistically significant relationship for the 28 d metrics of IVT (Table 1). However, we do find a statistically significant relationship for the 7 d metrics of IVT, with a probability of spurious correlation <2%. Hence, even though only 9 of the 41 events were associated with enhanced 7 d averaged metrics of IVT, this amount of events is unlikely to be caused by random chance and the correlation is statistically significant. This relationship is broadly consistent with Wille and others (2022), but applies to a wider set of ice shelves that span most of the Antarctic ice sheet.

Regional sensitivity to enhanced IVT

To determine if there are regional differences in the relationship between the metrics of IVT and iceberg calving, we separately applied our bootstrap to the calving events in the Antarctic Peninsula and the Amundsen Sea Embayment. These two regions experience contrasting meteorological and glaciological environments, and are the only regions that have enough events in our catalog to perform statistical tests. Our bootstrap shows that none of our metrics of IVT have a statistically significant relationship with calving events from the Amundsen Sea Embayment (Table 1). However, we do find a statistically significant relationship for the Antarctic Peninsula that mirrors that of our Antarctic-wide bootstrap: the 28 d metrics of IVT show no statistical significance, but we do see a statistically significant relationship between calving and both 7 d metrics of IVT.

Sensitivity to IVT threshold

It is possible that our results are sensitive to our chosen 90th percentile threshold that defines when metrics of IVT are considered 'enhanced'. To test this, we performed additional tests where we varied the threshold from the 80th to 95th percentiles (see Table 2). The sensitivity test bolsters our previous results: we find that for the ice-sheet-wide and the Antarctic Peninsula bootstrap both of our metrics of 7 d IVT remain statistically significant for thresholds that range from the 80th to 90th percentiles. For the Amundsen Sea Embayment, there is no consistent pattern of statistical significance for any threshold that we examined, although there are isolated metrics and thresholds that show significance. For example, IVT^{T}_{28} is the only metric statistically significant at the 85th percentile threshold, but IVT^{T}_{28} is not statistically significant for any other threshold we examined. Similarly, IVT^{V}_{28} for the Amundsen Sea Embayment was significant for the 95th percentile, but no other threshold. This suggests that our metrics of IVT show sensitivity to the choice of percentile threshold.

Discussion

Most calving events are not triggered by atmospheric moisture transport

Contrary to recent studies that suggest that extreme moisture transport acts as a trigger for calving (Francis and others, 2021, 2022; Wille and others, 2022, 2024), most of the calving events in our catalog are not associated with enhanced metrics of IVT (defined as the 90th percentile). This suggests that, at the very least, enhanced moisture transport is not a *necessary* condition to trigger tabular iceberg calving. Nonetheless, we do see a statistically significant fraction of calving events that are correlated with the 7 d metrics of IVT.

We also see regional differences in the statistical significance of the correlation between enhanced metrics of IVT and the timing of iceberg calving. For instance, the Antarctic Peninsula appears to show a relationship with statistical significance for both of the 7 d metrics of IVT, a result that holds whether we set the threshold for enhancement at the 85th or 90th percentile. This result is consistent with previous studies that show how extreme moisture transport over the Antarctic Peninsula was coincident with the rapid disintegration of the Larsen A and B ice shelves (Laffin and others, 2022; Wille and others, 2022). This pattern of statistical significance contrasts with our findings for the Amundsen Sea Embayment ice shelves, which do not appear to exhibit any consistent pattern showing a statistically significant correlation for any metrics of enhanced IVT. The discrepancy between these two regions is broadly consistent with ocean-driven retreat in the Amundsen Sea Embayment (Kimura and others, 2017; Nakayama and others, 2019).

It is possible that the regional differences between the Amundsen Sea Embayment and Antarctic Peninsula ice shelves extend to other ice shelves. However, the scarcity of calving events from the other ice shelves examined precludes a meaningful statistical analysis for most other regions unless we entertain geographically broad groupings, like all ice shelves that fringe the East Antarctic ice sheet. Given the difference between the Amundsen Sea Embayment and Antarctic Peninsula, however,

https://doi.org/10.1017/jog.2024.94 Published online by Cambridge University Press

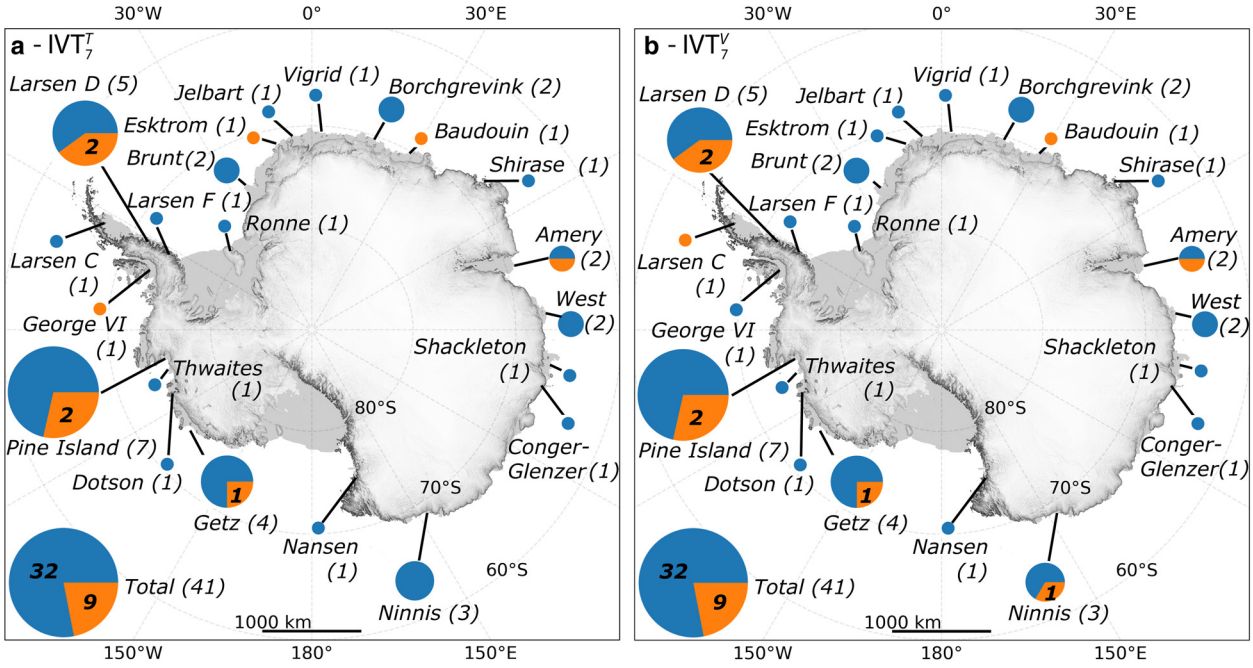

Figure 5. Calving events per ice shelf with the fraction of events that have enhanced 7 d IVT, shaded in orange, for (a) total IVT magnitude, IVT_7^T, and (b) meridional IVT, IVT_7^V. The radius of each circle is proportionate to the total number of calving events from the ice shelf associated with it. The total number of calving events from each ice shelf is listed beside the label for each circle. The numbers in each orange region are the counts of events with enhanced IVT_7^T or IVT_7^V. The total number of calving events is shown boxed in the lower left corner.

it seems likely that conditional factors that differ between regions – and perhaps individual ice shelves – that may result in greater sensitivity of tabular calving to enhanced IVT in some circumstances. Extending the time frame of our analysis to earlier than our 2013 start date could reveal additional regions that may be sensitive to enhanced IVT. On the other hand, because we compute monthly percentiles of the metrics of IVT from 1979 to 2023, trends in IVT over Antarctic ice shelves due to climate change may cause our study to overstate the statistical significance of the association of enhanced metrics of IVT with iceberg calving (Payne and others, 2020; Maclennan and others, 2023).

Attribution of calving triggers from case studies can be misleading

Our results also emphasize that caution is needed when evaluating statistical significance without physical mechanisms to link calving to specific choices of both metrics of IVT and thresholds on it. Previous studies linked calving events from the Amery, Brunt and Conger ice shelves to elevated conditions of anomalous atmospheric moisture transport (Francis and others, 2021, 2022; Wille and others, 2024). However, in our work, each of the calving events from those ice shelves corresponded to 7- and 28 d metrics of IVT that ranged from the 80th to the 89th percentiles, and were therefore not associated with enhanced IVT. This indicates that the moisture transport conditions over the ice shelves prior to their calving events examined by the case studies detailed in Francis and others (2021, 2022) and Wille and others (2024) are high (above the 80th percentile), but not particularly rare occurrences. Wille and others (2022) identified an atmospheric river prior to the July 2017 calving event from the Larsen C Ice Shelf, which in our study corresponded to enhanced IVT_{28}^V and IVT_7^V. Our results suggest that the connection between iceberg calving and atmospheric rivers found for the Antarctic Peninsula by Wille and others (2022) is limited to that region. Moreover, we found some metrics of IVT that resulted in isolated calving events being identified as coincident with 'enhanced' metrics of IVT, but no statistically significant relationship when applied to a larger set of calving events. Finally, because tabular calving typically has a much longer recurrence interval than enhanced IVT at the thresholds we examined, most incidences of enhanced IVT over the ice shelves we examined are not coincident with calving. This suggests that correlation between calving and IVT we observed may have little predictive power. For instance, as we decrease the percentile threshold, we also observe a much larger number of enhanced IVT events that are not associated with any calving event. For example, the Ronne Ice Shelf saw at least 80th percentile IVT_7^T 92 times from 2013 to 2023, compared to 49 instances of 90th percentile IVT_7^T over the same ice shelf. This is still much more frequent than the number of calving events from the Ronne Ice Shelf, which occurred only once in the study period. Therefore, while enhanced IVT may be significantly correlated with the timing of calving for a minority of the calving events, it still may have low predictive power in determining when iceberg calving events occur. This is consistent with the fact that, at least at the 90th percentile, ~80% of calving events are not associated with any enhanced metrics of IVT. As we decrease the threshold, the number of events associated with metrics of IVT increase, but so do the number of instances

Table 1. Number of calving events in the catalog that have enhanced IVT^T and IVT^V, both for Antarctic-wide events, and those from the respective Amundsen Sea Embayment and the Antarctic Peninsula regions

	Antarctic-wide (41 events)		Amundsen Sea Embayment (13 events)		Antarctic Peninsula (8 events)	
	28 d	7 d	28 d	7 d	28 d	7 d
IVT^T	6 (30%)	9 **(2%)**	3 (14%)	3 (14%)	2 (23%)	3 **(4%)**
IVT^V	6 (25%)	9 **(2%)**	2 (29%)	3 (13%)	3 (8%)	3 **(4%)**

The probability of spurious correlation between real events and enhanced metrics of IVT is given in parentheses beside each count. Reported probabilities are rounded to the nearest integer percentage. Percent values below 5% (i.e. those considered significant at the 95% level) are bolded.

https://doi.org/10.1017/jog.2024.94 Published online by Cambridge University Press

Table 2. Number of calving events that have IVT^T and IVT^V that exceeds the 80th, 85th, 90th and 95th percentiles for those in the Amundsen Sea Embayment and the Antarctic Peninsula

	80th		85th		90th		95th	
	28 d	7 d	28 d	7 d	28 d	7 d	28 d	7 d
Amundsen Sea Embayment								
IVT^T	6 **(3%)**	3 (50%)	4 (14%)	3 (31%)	3 (14%)	3 (14%)	2 (8%)	2 (13%)
IVT^V	5 (8%)	4 (25%)	5 **(2%)**	3 (32%)	2 (28%)	3 (13%)	2 (8%)	3 **(2%)**
Antarctic Peninsula								
IVT^T	3 (20%)	5 **(1%)**	3 (12%)	5 **(0%)**	2 (23%)	3 **(4%)**	2 (8%)	1 (33%)
IVT^V	6 **(0%)**	4 (6%)	3 (14%)	4 **(2%)**	3 (8%)	3 **(4%)**	1 (50%)	2 (6%)

The probability of spurious correlation between real events and enhanced metrics of IVT (as defined at each percentile threshold) is given in parentheses beside each count. Reported probabilities are rounded to the nearest integer percentage. Percent values below 5% (i.e. those considered significant at the 95% level) are bolded.

when IVT exceeds the threshold without a simultaneous calving event.

It is also possible that, although enhanced IVT itself has little predictive power, the correlation with calving is statistically significant because IVT covaries with other environmental variables that may have a more direct mechanical connection to the calving process. For instance, enhanced IVT is connected with warm air advection and consequently anomalously high temperatures, which can result in surface melt (Bozkurt and others, 2018; Wille and others, 2019; Adusumilli and others, 2021; Djoumna and Holland, 2021; Gorodetskaya and others, 2023). Enhanced IVT is also associated with conditions that result in higher wind speeds, sea surface slopes and sea ice clearing, which have also been hypothesized to impact iceberg calving (Arthur and others, 2021; Francis and others, 2021, 2022; Wille and others, 2024). Our study can only determine if the observed correlation between enhanced metrics of IVT and calving is statistically significant and does not inform us about the potential causal mechanisms that link enhanced IVT to calving.

Our methodology can be extended to other environmental triggers

The methodology we applied here can be applied to a variety of potential triggers. For example, Table 3 shows the results of our bootstrap applied to the 10 m wind speed and 2 m atmospheric temperature using a 90th percentile threshold. We see no statistically significant correlation between calving and wind speed. However, we do see a statistically significant correlation with 2 m temperature. Here we see that all calving events that have enhanced IVT also have enhanced 2 m temperature. At first glance, the connection between calving and atmospheric temperature is not surprising given the link between surface melt and hydrofracture (Scambos and others, 2000; van den Broeke, 2005; Robel and Banwell, 2019). However, the correlation we see is apparent through analysis of synoptic- to up to weekly-scale variations of temperature. This diverges from current theory which suggests sensitivity of ice shelves to surface melt and hydrofracture requires longer-term depletion of firn-air content (Kuipers Munneke and others, 2014; Machguth and others, 2016; Robel and Banwell, 2019). Given the potential for biases in ERA 2 m temperatures, and the fact that the correlation between calving and temperature may also not be causal, we view this connection between 2 m temperature and calving as it appears here as speculative. Nonetheless, it illustrates that we can begin to perform more systematic attribution studies given a large enough catalog of icebergs.

Table 3. Number of calving events that have enhanced 2 m temperature and 10 m wind speed for each in the catalog, both Antarctic-wide, and for the events from ice shelves surrounding the Amundsen Sea Embayment, and the Antarctic Peninsula

	Antarctic-wide (41 events)		Amundsen Sea Embayment (13 events)		Antarctic Peninsula (8 events)	
	28 d	7 d	28 d	7 d	28 d	7 d
2 m temperature	15 **(0%)**	11 **(0%)**	7 **(0%)**	4 **(4%)**	2 (47%)	3 (5%)
10 m wind speed	7 (11%)	3 (79%)	1 (69%)	1 (73%)	1 (68%)	1 (69%)

The probabilities of spurious correlations between real events and enhanced 2 m temperature and 10 m wind speed are given in parentheses beside each count. Reported probabilities are rounded to the nearest integer percentage. Percent values below 5% (i.e. those considered significant at the 95% level) are bolded.

Conclusions

We investigated the extent by which enhanced atmospheric water vapor transport over Antarctic ice shelves is correlated with tabular iceberg calving events by examining metrics of IVT derived from ERA5 reanalysis. We found that a majority of calving events (~80%) are not associated with any of our metrics of enhanced IVT. However, the fraction of tabular iceberg calving events that had enhanced metrics of 7 d IVT occurred at a greater frequency than would be expected solely from the climatology if no relationship existed. This correlation was statistically significant when applied either continent-wide or to the Antarctic Peninsula specifically. The relationship was insensitive to specific definitions of the 7 d metric or threshold used to define 'enhanced'. By contrast, we saw no statistically significant correlation between metrics of enhanced IVT and ice shelves in the Amundsen Sea Embayment, suggesting that triggers for iceberg calving are, not surprisingly, regionally-specific.

Antarctic ice shelves are expected to become more vulnerable to atmospheric air temperature extremes through the 21st century, particularly in ice shelves in typically dry regions (Gilbert and Kittel, 2021; van Wessem and others, 2023). Furthermore, atmospheric rivers in the future are expected to become more frequent and intense (Payne and others, 2020; Maclennan and others, 2023). Therefore, it is likely that we will see more icebergs that detach during periods when enhanced atmospheric moisture transport is occurring. However, because calving events occur much less frequently than any of our enhanced metrics of IVT, it seems unlikely IVT is the primary driver of calving events. Instead, it seems more likely that when ice shelves evolve into a state where rifts nearly isolate an iceberg, the timing of the final calving event shows increased sensitivity to modest levels of IVT. This would imply that, although the mechanical impact of enhanced IVT, sea slope, winds and other variables is small most of the time (e.g. Bassis and others, 2008), as ice shelves become more fractured and rifts come closer to isolating icebergs, these variables become more important. If this is the case, then as ice shelves continue to evolve under future climate warming, we are likely to see more ice shelves preconditioned to be more

https://doi.org/10.1017/jog.2024.94 Published online by Cambridge University Press

sensitive to enhanced IVT or other environmental forcing. However, it is the processes governing preconditioning that will control the future stability of ice shelves.

Tabular iceberg calving is a sporadic process on Antarctic ice shelves that can have minimal impact on the mass balance of the Antarctic ice sheet at the present (Fricker and others, 2002; Bassis and others, 2024). However, if the mass removed by the calving event reduces the buttressing force on the Antarctic ice sheet due to the ice shelf, accelerated mass flux across the grounding line of the ice sheet can increase discharge into the oceans (Dupont and Alley, 2005; Gudmundsson and others, 2019; Marsh and others, 2024). The increased mass flux into the ocean can raise the net contribution of the Antarctic ice sheet to the rate of sea-level rise. However, increased atmospheric water vapor transport and more frequent atmospheric river landfalls across the ice sheet can increase the amount of snowfall, effectively offsetting mass losses through the ice shelves (Wille and others, 2021; Davison, 2023; Maclennan and others, 2023; Park and others, 2023; Rendfrey and others, 2024). Furthermore, although we have found that connection between enhanced IVT and calving is, at best, weak, it is possible that there is a stronger connection with ice shelf rift propagation that precedes calving. Alternative methods to describe change on the ice sheet, for example, the detection of crevasses and their evolution described in Li and others (2024) could be applied in conjunction with analysis of enhanced atmospheric water vapor transport in future work. However, our study remains limited to assessing correlation and still cannot determine causality, which requires a physical mechanism linking atmospheric extremes to calving or rift propagation. The diverging potential consequences of enhanced atmospheric moisture transport on Antarctic surface processes therefore remains a large source of uncertainty in projections of Antarctic ice sheet mass balance and, consequently, future rates of sea-level rise. Further investigation of the physical processes linking enhanced atmospheric moisture transport to surface conditions on Antarctic ice shelves may contribute to reducing such uncertainty.

Supplementary material. The supplementary material for this article can be found at https://doi.org/10.1017/jog.2024.94.

Acknowledgments. This work is funded by DoE grant C3710, Framework for Antarctic System Science in E3SM, NASA grant 80NSSC22K0378 and by the DOMINOS project, a component of the International Thwaites Glacier Collaboration (ITGC), with support from National Science Foundation (NSF: grant 1738896) and Natural Environment Research Council (NERC: grant NE/S006605/1).

References

Adusumilli S, Fish M, Fricker HA and Medley B (2021) Atmospheric river precipitation contributed to rapid increases in surface height of the West Antarctic ice sheet in 2019. *Geophysical Research Letters* **48**(5), e2020GL091076. doi: 10.1029/2020GL091076

Alley R and 8 others (2023) Iceberg calving: regimes and transitions. *Annual Review of Earth and Planetary Sciences* **51**(1), 189–215. doi: 10.1146/annurev-earth-032320-110916

Amundson JM and Truffer M (2010) A unifying framework for iceberg-calving models. *Journal of Glaciology* **56**(199), 822–830. doi: 10.3189/002214310794457173

Arthur JF and 5 others (2021) The triggers of the disaggregation of Voyeykov ice shelf (2007), Wilkes Land, East Antarctica, and its subsequent evolution. *Journal of Glaciology* **67**(265), 933–951. doi: 10.1017/jog.2021.45

Banwell AF, MacAyeal DR and Sergienko OV (2013) Breakup of the Larsen B ice shelf triggered by chain reaction drainage of supraglacial lakes. *Geophysical Research Letters* **40**(22), 5872–5876. doi: 10.1002/2013gl057694

Bassis JN and 9 others (2024) Stability of ice shelves and ice cliffs in a changing climate. *Annual Review of Earth and Planetary Sciences* **52**(1), 221-247. doi: 10.1146/annurev-earth-040522-122817

Bassis JN and Jacobs S (2013) Diverse calving patterns linked to glacier geometry. *Nature Geoscience* **6**(10), 833–836. doi: 10.1038/ngeo1887

Bassis JN and Walker CC (2011) Upper and lower limits on the stability of calving glaciers from the yield strength envelope of ice. *Proceedings of the Royal Society A: Mathematical, Physical and Engineering Sciences* **468**(2140), 913–931. doi: 10.1098/rspa.2011.0422

Bassis JN, Fricker HA, Coleman R and Minster JB (2008) An investigation into the forces that drive ice-shelf rift propagation on the Amery ice shelf, East Antarctica. *Journal of Glaciology* **54**(184), 17–27. doi: 10.3189/002214308784409116

Benn DI and 10 others (2022) Rapid fragmentation of Thwaites Eastern ice shelf. *The Cryosphere* **16**(6), 2545–2564. doi: 10.5194/tc-16-2545-2022

Bozkurt D, Rondanelli R, Marín JC and Garreaud R (2018) Foehn event triggered by an atmospheric river underlies record-setting temperature along continental Antarctica. *Journal of Geophysical Research: Atmospheres* **123**(8), 3871–3892. doi: 10.1002/2017JD027796

Bozkurt D, Marín JC and Barrett BS (2022) Temperature and moisture transport during atmospheric blocking patterns around the Antarctic Peninsula. *Weather and Climate Extremes* **38**, 100506. doi: 10.1016/j.wace.2022.100506

Bromirski PD, Sergienko OV and MacAyeal DR (2010) Transoceanic infragravity waves impacting Antarctic ice shelves. *Geophysical Research Letters* **37**(2), L02502. doi: 10.1029/2009GL041488

Budge JS and Long DG (2018) A comprehensive database for Antarctic iceberg tracking using scatterometer data. *IEEE Journal of Selected Topics in Applied Earth Observations and Remote Sensing* **11**(2), 434–442. doi: 10.1109/jstars.2017.2784186

Camuffo D, Becherini F, della Valle A (2020) Relationship between selected percentiles and return periods of extreme events. *Acta Geophysica* **68**(4), 1201–1211. doi: 10.1007/s11600-020-00452-x

Clem KR, Bozkurt D, Kennett D, King JC and Turner J (2022) Central tropical pacific convection drives extreme high temperatures and surface melt on the Larsen C ice shelf, Antarctic Peninsula. *Nature Communications* **13**(1). doi: 10.1038/s41467-022-31119-4

Costi J and 7 others (2018) Estimating surface melt and runoff on the Antarctic Peninsula using ERA-Interim reanalysis data. *Antarctic Science* **30**(6), 379–393. doi: 10.1017/s0954102018000391

Crosson WL, Al-Hamdan MZ, Hemmings SNJ and Wade GM (2012) A daily merged MODIS Aqua–Terra land surface temperature data set for the conterminous United States. *Remote Sensing of Environment* **119**, 315–324. doi: 10.1016/j.rse.2011.12.019

Davison BJ and 8 others (2023) Annual mass budget of Antarctic ice shelves from 1997 to 2021. *Science Advances* **9**(41). doi: 10.1126/sciadv.adi0186

Davison BJ (2023) Sea level rise from West Antarctic mass loss significantly modified by large snowfall anomalies. *Nature Communications* **14**(1479). doi: 10.1038/s41467-023-36990-3

DeConto RM and Pollard D (2016) Contribution of Antarctica to past and future sea-level rise. *Nature* **531**(7596), 591–597. doi: 10.1038/nature17145

Depoorter MA and 6 others (2013) Calving fluxes and basal melt rates of Antarctic ice shelves. *Nature* **502**(7469), 89–92. doi: 10.1038/nature12567

Djoumna G and Holland DM (2021) Atmospheric rivers, warm air intrusions, and surface radiation balance in the Amundsen Sea Embayment. *Journal of Geophysical Research: Atmospheres* **126**(13). doi: 10.1029/2020JD034119

Dupont TK and Alley RB (2005) Assessment of the importance of ice-shelf buttressing to ice-sheet flow. *Geophysical Research Letters* **32**(4), L04503. doi: 10.1029/2004gl022024

Dziak RP and 10 others (2019) Hydroacoustic, meteorologic and seismic observations of the 2016 Nansen ice shelf calving event and iceberg formation. *Frontiers in Earth Science* **7**. doi: 10.3389/feart.2019.00183

Edwards TL and 9 others (2019) Revisiting Antarctic ice loss due to marine ice-cliff instability. *Nature* **566**(7742), 58–64. doi: 10.1038/s41586-019-0901-4

Efron B (1979) Computers and the theory of statistics: thinking the unthinkable. *SIAM Review* **21**(4), 460–480. doi: 10.1137/1021092

England MR, Wagner TJW and Eisenman I (2020) Modeling the breakup of tabular icebergs. *Science Advances* **6**(51), eabd1273. doi: 10.1126/sciadv.abd1273

Espinoza V, Waliser DE, Guan B, Lavers DA and Ralph FM (2018) Global analysis of climate change projection effects on atmospheric rivers. *Geophysical Research Letters* **45**(9), 4299–4308. doi: 10.1029/2017gl076968

Francis D and 5 others (2022) Atmospheric triggers of the Brunt ice shelf calving in February 2021. *Journal of Geophysical Research: Atmospheres* **127**(11), e2021JD036424. doi: 10.1029/2021jd036424

Francis D, Mattingly KS, Lhermitte S, Temimi M and Heil P (2021) Atmospheric extremes caused high oceanward sea surface slope triggering the biggest calving event in more than 50 years at the Amery ice shelf. *The Cryosphere* **15**(5), 2147–2165. doi: 10.5194/tc-15-2147-2021

Fricker HA, Young NW, Allison I and Coleman R (2002) Iceberg calving from the Amery ice shelf, East Antarctica. *Annals of Glaciology* **34**, 241–246. doi: 10.3189/172756402781817581

Gagliardini O, Durand G, Zwinger T, Hindmarsh RCA and Le Meur E (2010) Coupling of ice-shelf melting and buttressing is a key process in ice-sheets dynamics. *Geophysical Research Letters* **37**(14), L14501. doi: 10.1029/2010gl043334

Garbe J, Albrecht T, Levermann A, Donges JF and Winkelmann R (2020) The hysteresis of the Antarctic ice sheet. *Nature* **585**(7826), 538–544. doi: 10.1038/s41586-020-2727-5

Gilbert E and Kittel C (2021) Surface melt and runoff on Antarctic ice shelves at 1.5°C, 2°C, and 4°C of future warming. *Geophysical Research Letters* **48**(8), e2020GL091733. doi: 10.1029/2020gl091733

Gimeno L, Nieto R, Vazquez M and Lavers DA (2014) Atmospheric rivers: a mini-review. *Frontiers in Earth Science* **2**. doi: 10.3389/feart.2014.00002

Glasser N and Scambos T (2008) A structural glaciological analysis of the 2002 Larsen B ice-shelf collapse. *Journal of Glaciology* **54**(184), 3–16. doi: 10.3189/002214308784409017

Goldberg D, Holland DM and Schoof C (2009) Grounding line movement and ice shelf buttressing in marine ice sheets. *Journal of Geophysical Research: Earth Surface* **114**(F4), F04026. doi: 10.1029/2008jf001227

Gorodetskaya IV and 5 others (2014) The role of atmospheric rivers in anomalous snow accumulation in East Antarctica. *Geophysical Research Letters* **41**(17), 6199–6206. doi: 10.1002/2014GL060881

Gorodetskaya IV and 24 others (2023) Record-high Antarctic Peninsula temperatures and surface melt in February 2022: a compound event with an intense atmospheric river. *npj Climate and Atmospheric Science* **6**(1). doi: 10.1038/s41612-023-00529-6

Greene CA, Gardner AS, Schlegel NJ and Fraser AD (2022) Antarctic calving loss rivals ice-shelf thinning. *Nature* **609**(7929), 948–953. doi: 10.1038/s41586-022-05037-w

Gudmundsson GH (2013) Ice-shelf buttressing and the stability of marine ice sheets. *The Cryosphere* **7**(2), 647–655. doi: 10.5194/tc-7-647-2013

Gudmundsson GH, Paolo FS, Adusumilli S and Fricker HA (2019) Instantaneous Antarctic ice sheet mass loss driven by thinning ice shelves. *Geophysical Research Letters* **46**(23), 13903–13909. doi: 10.1029/2019GL085027

Hersbach H and 42 others (2020) The ERA5 global reanalysis. *Quarterly Journal of the Royal Meteorological Society* **146**(730), 1999–2049. doi: 10.1002/qj.3803

Humbert A and Steinhage D (2011) The evolution of the western rift area of the Fimbul Ice Shelf, Antarctica. *The Cryosphere* **5**(4), 931–944. doi: 10.5194/tc-5-931-2011

Indrigo C, Dow CF, Greenbaum JS and Morlighem M (2020) Drygalski ice tongue stability influenced by rift formation and ice morphology. *Journal of Glaciology* **67**(262), 243–252. doi: 10.1017/jog.2020.99

Joughin I and MacAyeal DR (2005) Calving of large tabular icebergs from ice shelf rift systems. *Geophysical Research Letters* **32**(2), L02501. doi: 10.1029/2004gl020978

Kenneally J and Hughes T (2006) Calving giant icebergs: old principles, new applications. *Antarctic Science* **18**(3), 409–419. doi: 10.1017/s0954102006000459

Kimura S and 9 others (2017) Oceanographic controls on the variability of ice-shelf basal melting and circulation of glacial meltwater in the Amundsen Sea Embayment, Antarctica. *Journal of Geophysical Research: Oceans* **122**(12), 10131–10155. doi: 10.1002/2017jc012926

Kuipers Munneke P and 12 others (2018) Intense winter surface melt on an Antarctic ice shelf. *Geophysical Research Letters* **45**(15), 7615–7623. doi: 10.1029/2018gl077899

Kuipers Munneke P, Picard G, van den Broeke MR, Lenaerts JTM and van Meijgaard E (2012) Insignificant change in Antarctic snowmelt volume since 1979. *Geophysical Research Letters* **39**(1), L01501. doi: 10.1029/2011gl050207

Kuipers Munneke P, Ligtenberg SR, van den Broeke MR and Vaughan DG (2014) Firn air depletion as a precursor of Antarctic ice-shelf collapse. *Journal of Glaciology* **60**(220), 205–214. doi: 10.3189/2014jog13j183

Laffin MK, Zender CS, van Wessem M and Marinsek S (2022) The role of föhn winds in eastern Antarctic Peninsula rapid ice shelf collapse. *The Cryosphere* **16**(4), 1369–1381. doi: 10.5194/tc-16-1369-2022

Lazzara MA, Jezek KC, Scambos TA, MacAyeal DR and van der Veen CJ (1999) On the recent calving of icebergs from the Ross Ice Shelf. *Polar Geography* **23**(3), 201–212. doi: 10.1080/10889379909377676

Legrésy B, Wendt A, Tabacco I, Rémy F and Dietrich R (2004) Influence of tides and tidal current on Mertz Glacier, Antarctica. *Journal of Glaciology* **50**(170), 427–435. doi: 10.3189/172756504781829828

Lenaerts JTM, Medley B, van den Broeke MR and Wouters B (2019) Observing and modeling ice sheet surface mass balance. *Reviews of Geophysics* **57**(2), 376–420. doi: 10.1029/2018rg000622

Lescarmontier L and 6 others (2015) Rifting processes and ice-flow modulation observed on Mertz Glacier, East Antarctica. *Journal of Glaciology* **61**(230), 1183–1193. doi: 10.3189/2015JoG15J028

Li Q and 7 others (2024) Three-dimensional dynamic monitoring of crevasses based on deep learning and surface elevation reconstruction methods. *International Journal of Applied Earth Observation and Geoinformation* **132**, 104017. doi: 10.1016/j.jag.2024.104017

Lipovsky BP (2020) Ice shelf rift propagation: stability, three-dimensional effects, and the role of marginal weakening. *The Cryosphere* **14**(5), 1673–1683. doi: 10.5194/tc-14-1673-2020

Liu Y and 7 others (2015) Ocean-driven thinning enhances iceberg calving and retreat of Antarctic ice shelves. *Proceedings of the National Academy of Sciences* **112**(11), 3263–3268. doi: 10.1073/pnas.1415137112

MacAyeal DR and 13 others (2006) Transoceanic wave propagation links iceberg calving margins of Antarctica with storms in tropics and Northern Hemisphere. *Geophysical Research Letters* **33**(17), L17502. doi: 10.1029/2006GL027235

Machguth H and 9 others (2016) Greenland meltwater storage in firn limited by near-surface ice formation. *Nature Climate Change* **6**(4), 390–393. doi: 10.1038/nclimate2899

Maclennan ML and 9 others (2023) Climatology and surface impacts of atmospheric rivers on West Antarctica. *The Cryosphere* **17**(2), 865–881. doi: 10.5194/tc-17-865-2023

Marsh OJ, Luckman AJ and Hodgson DA (2024) Brief Communication: Rapid acceleration of the Brunt Ice Shelf after calving of iceberg A-81. *The Cryosphere* **18**(2), 705–710. doi: 10.5194/tc-18-705-2024

Massom RA and 5 others (2018) Antarctic ice shelf disintegration triggered by sea ice loss and ocean swell. *Nature* **558**(7710), 383–389. doi: 10.1038/s41586-018-0212-1

Mayet C, Testut L, Legresy B, Lescarmontier L and Lyard F (2013) High-resolution barotropic modeling and the calving of the Mertz Glacier, East Antarctica. *Journal of Geophysical Research: Oceans* **118**(10), 5267–5279. doi: 10.1002/jgrc.20339

Miles BWJ and 5 others (2022) High spatial and temporal variability in Antarctic ice discharge linked to ice shelf buttressing and bed geometry. *Scientific Reports* **12**(1), 10968. doi: 10.1038/s41598-022-13517-2

Mouginot J (2017) Measures Antarctic boundaries for IPY 2007–2009 from satellite radar, version 2. doi: 10.5067/AXE4121732AD

Nakayama Y and 9 others (2019) Pathways of ocean heat towards Pine Island and Thwaites grounding lines. *Scientific Reports* **9**(1), 16649. doi: 10.1038/s41598-019-53190-6

Nash D, Waliser D, Guan B, Ye H and Ralph FM (2018) The role of atmospheric rivers in extratropical and polar hydroclimate. *Journal of Geophysical Research: Atmospheres* **123**(13), 6804–6821. doi: 10.1029/2017jd028130

Nicolas JP and Bromwich DH (2011) Climate of West Antarctica and influence of marine air intrusions. *Journal of Climate* **24**(1), 49–67. doi: 10.1175/2010jcli3522.1

Paolo FS, Fricker HA and Padman L (2015) Volume loss from Antarctic ice shelves is accelerating. *Science* **348**(6232), 327–331. doi: 10.1126/science.aaa0940

Park JY and 5 others (2023) Future sea-level projections with a coupled atmosphere–ocean–ice-sheet model. *Nature Communications* **14**(1). doi: 10.1038/s41467-023-36051-9

Payne AE and 9 others (2020) Responses and impacts of atmospheric rivers to climate change. *Nature Reviews Earth and Environment* **1**(3), 143–157. doi: 10.1038/s43017-020-0030-5

Pollard D, DeConto RM and Alley RB (2015) Potential Antarctic ice sheet retreat driven by hydrofracturing and ice cliff failure. *Earth and Planetary Science Letters* **412**, 112–121. doi: 10.1016/j.epsl.2014.12.035

Rendfrey TS, Pettersen C, Bassis JN and Mateling ME (2024) CloudSat observations show enhanced moisture transport events increase snowfall rate and frequency over Antarctic ice sheet basins. *Journal of Geophysical Research: Atmospheres* **129**(6), e2023JD040556. doi: 10.1029/2023JD040556

https://doi.org/10.1017/jog.2024.94 Published online by Cambridge University Press

Rignot E (2002) Ice-shelf changes in Pine Island Bay, Antarctica, 1947–2000. *Journal of Glaciology* **48**(161), 247–256. doi: 10.3189/172756502781831386

Rignot E and 5 others (2019) Four decades of Antarctic ice sheet mass balance from 1979–2017. *Proceedings of the National Academy of Sciences* **116**(4), 1095–1103. doi: 10.1073/pnas.1812883116

Robel AA and Banwell AF (2019) A speed limit on ice shelf collapse through hydrofracture. *Geophysical Research Letters* **46**(21), 12092–12100. doi: 10.1029/2019gl084397

Robin GDQ (1979) Formation, flow, and disintegration of ice shelves. *Journal of Glaciology* **24**(90), 259–271. doi: 10.3189/s0022143000014787

Scambos TA, Hulbe C, Fahnestock M and Bohlander J (2000) The link between climate warming and break-up of ice shelves in the Antarctic Peninsula. *Journal of Glaciology* **46**(154), 516–530. doi: 10.3189/172756500781833043

Schlemm T and Levermann A (2021) A simple parametrization of mélange buttressing for calving glaciers. *The Cryosphere* **15**(2), 531–545. doi: 10.5194/tc-15-531-2021

Sergienko OV (2010) Elastic response of floating glacier ice to impact of long-period ocean waves. *Journal of Geophysical Research: Earth Surface* **115**(F4), F04028. doi: 10.1029/2010JF001721

Shields CA, Wille JD, Marquardt Collow AB, Maclennan M and Gorodetskaya IV (2022) Evaluating uncertainty and modes of variability for Antarctic atmospheric rivers. *Geophysical Research Letters* **49**(16), e2022GL099577. doi: 10.1029/2022gl099577

Swetha Chittella SP, Deb P and Melchior van Wessem J (2022) Relative contribution of atmospheric drivers to 'extreme' snowfall over the Amundsen Sea Embayment. *Geophysical Research Letters* **49**(16), e2022GL098661. doi: 10.1029/2022gl098661

Terpstra A, Gorodetskaya IV and Sodemann H (2021) Linking sub-tropical evaporation and extreme precipitation over East Antarctica: an atmospheric river case study. *Journal of Geophysical Research: Atmospheres* **126**(9), e2020JD033617. doi: 10.1029/2020jd033617

Trusel LD, Frey KE, Das SB, Munneke PK, van den Broeke MR (2013) Satellite-based estimates of Antarctic surface meltwater fluxes. *Geophysical Research Letters* **40**(23), 6148–6153. doi: 10.1002/2013gl058138

Turton JV, Kirchgaessner A, Ross AN, King JC and Kuipers Munneke P (2020) The influence of föhn winds on annual and seasonal surface melt on the Larsen C Ice Shelf, Antarctica. *The Cryosphere* **14**(11), 4165–4180. doi: 10.5194/tc-14-4165-2020

van den Broeke M (2005) Strong surface melting preceded collapse of Antarctic Peninsula ice shelf. *Geophysical Research Letters* **32**(12), L12815. doi: 10.1029/2005gl023247

van Wessem JM, van den Broeke MR, Wouters B and Lhermitte S (2023) Variable temperature thresholds of melt pond formation on Antarctic ice shelves. *Nature Climate Change* **13**(2), 161–166. doi: 10.1038/s41558-022-01577-1

Walker CC, Bassis JN, Fricker HA and Czerwinski RJ (2013) Structural and environmental controls on Antarctic ice shelf rift propagation inferred from satellite monitoring. *Journal of Geophysical Research: Earth Surface* **118**(4), 2354–2364. doi: 10.1002/2013JF002742

Walker CC, Bassis JN, Fricker HA and Czerwinski RJ (2015) Observations of interannual and spatial variability in rift propagation in the Amery Ice Shelf, Antarctica, 2002–14. *Journal of Glaciology* **61**(226), 243–252. doi: 10.3189/2015jog14j151

Walker CC, Becker MK and Fricker HA (2021) A high resolution, three-dimensional view of the D-28 calving event from Amery Ice Shelf with ICESat-2 and satellite imagery. *Geophysical Research Letters* **48**(3), e2020GL091200. doi: 10.1029/2020gl091200

Wilks DS (2011) *Statistical Methods in the Atmospheric Sciences*. Oxford: Academic Press.

Wille JD and 6 others (2019) West Antarctic surface melt triggered by atmospheric rivers. *Nature Geoscience* **12**(11), 911–916. doi: 10.1038/s41561-019-0460-1

Wille JD and 8 others (2021) Antarctic atmospheric river climatology and precipitation impacts. *Journal of Geophysical Research: Atmospheres* **126**(8), e2020JD033788. doi: 10.1029/2020jd033788

Wille JD and 14 others (2022) Intense atmospheric rivers can weaken ice shelf stability at the Antarctic Peninsula. *Communications Earth and Environment* **3**(1). doi: 10.1038/s43247-022-00422-9

Wille JD and 53 others (2024) The extraordinary March 2022 East Antarctica 'heat' wave. Part II: impacts on the Antarctic ice sheet. *Journal of Climate* **37**(3), 779–799. doi: 10.1175/jcli-d-23-0176.1

Xiong X and Barnes W (2006) An overview of MODIS radiometric calibration and characterization. *Advances in Atmospheric Sciences* **23**(1), 69–79. doi: 10.1007/s00376-006-0008-3

https://doi.org/10.1017/jog.2024.94 Published online by Cambridge University Press